

## EFFECT OF TENSILE FORCE FOR WEAR PERFORMANCE OF MOORING CHAIN

Gotoh, Koji

Department of Marine Systems Engineering, Faculty of Engineering, Kyushu University

Nakagawa, Masataka

Department of Civil and Structural Engineering, Graduate School of Engineering, Kyushu University : Master course student

Murakami, Koji

Department of Civil and Structural Engineering, Graduate school of Engineering, Kyushu University

Utsunomiya, Tomoaki

Department of Marine Systems Engineering, Faculty of Engineering, Kyushu University

<https://hdl.handle.net/2324/4753060>

---

出版情報 : Proceedings of the ASME 2018 37th International Conference on Ocean, Offshore and Arctic Engineering: OMAE2018, 2018-09-25. The American Society of Mechanical Engineers : ASME  
バージョン :  
権利関係 : Copyright © 2017 by ASME



**OMAE2018-77960**

**EFFECT OF TENSILE FORCE FOR WEAR PERFORMANCE OF MOORING CHAIN**

**Koji Gotoh**

Department of Marine Systems Engineering,  
Faculty of Engineering,  
Kyushu University  
744 Motooka, Nishi-ku, Fukuoka  
819-0395, Japan  
Tel: +81-92-802-3457  
Fax: +81-92-802-3368  
E-mail: gotoh@nams.kyushu-u.ac.jp

**Masataka Nakagawa**

Master course student,  
Department of Civil and Structural Engineering,  
Graduate school of Engineering,  
Kyushu University  
744 Motooka, Nishi-ku, Fukuoka  
819-0395, Japan  
Tel: +81-92-802-3464  
Fax: +81-92-802-3368  
Email: 2TE16294N@s.kyushu-u.ac.jp

**Koji Murakami**

Department of Civil and Structural Engineering,  
Graduate School of Engineering,  
Kyushu University  
744 Motooka, Nishi-ku, Fukuoka  
819-0395, Japan  
Tel: +81-92-802-3464  
Fax: +81-92-802-3368  
Email: murakami@nams.kyushu-u.ac.jp

**Tomoaki Utsunomiya**

Department of Marine Systems Engineering,  
Faculty of Engineering,  
Kyushu University  
744 Motooka, Nishi-ku, Fukuoka  
819-0395, Japan  
Tel: +81-92-802-3447  
Fax: +81-92-802-3368  
Email: utsunomiya@nams.kyushu-u.ac.jp

**ABSTRACT**

Floating wind turbine facilities, which are installed in the deep sea area, plays an essential role to promote the green energy application. One of the problems associated with the commercialization of facilities installed in the deep sea is the reduction of the maintenance cost of mooring chain, because breaking of the mooring chain caused by the wear between links leads to enormous economic losses. Therefore, it is necessary to establish a quantitative wear evaluation method for mooring chains.

Experimental facility to reproduce the wear caused by sliding between links in actual scale applied for floating wind turbine, which had been proposed by the authors, was updated and the wear tests was conducted by setting some tensile force conditions between the links. Besides, procedure of the nonlinear finite element analysis was improved to estimate the behaviour of wearing between links.

From experiments and numerical analysis, it has been confirmed that the tensile force between links is an important factor of the wear amount between links.

**INTRODUCTION**

To reduce the emission of medium and long term greenhouse gas, it is necessary to promote the application of renewable energy instead of the fossil fuel. The wind power generation is expected to play in meeting this goal. The implementation of offshore wind power generation is advantageous because it is capable of stable and efficient power generation due to the strong wind speed whose variation on offshore is small. To spread the wind power generation plant on offshore over the world, the floating wind turbine facilities in the deep sea area is essential.

One of the issues related to the practical application of the commercialized deep sea facility is the reduction of a mooring cost. As of the cases reported in the buoys installed in the port, mooring chain of floating body was damaged due to wear caused by its motion [1]. If the floating wind power turbine installed in the deep sea area cannot be moored due to the breaking of mooring chain by wear, it will cause the serious impact on the power generation. It is essential to establish quantitative evaluation of the wear performance of mooring chain of in-service since only visual inspection by divers or ROV is available in the present.

In relation to the wear performance of mooring chain, Yaghin and Melchers [2] reported wear test results for chain consists of Stud link with the cross section diameter 16mm. In these tests, the chain motion to cause the wear was produced by considering the behaviour of mooring chain connected to the floating production storage and off-loading (FPSO) vessels. They confirm that tensile force working between the links has a significant but non-linear effect on the inter-link wear. Their experiments were, however, slightly small scale and they did not mention the estimation procedure of the amount of wear. Brown et al. [3] proposed a practical method to estimate wear and corrosion of mooring chains based on calibration with field measurements. However, the estimate from this method is dependent on the calibration determined from the specific moored area.

We had proposed experimental facility and numerical procedure to reproduce the inter-link wear in actual scale [4]. However, we only reported the experimental and numerical result under one tensile and sliding angle condition because of the limitation of tensile loading between links and insufficient study on finite element modelling.

In this study, we developed the experimental facility and finite element analysis procedure to reproduce the inter-link wear in actual scale and investigated the effect of inter-link tensile force on the wear performance.

## IMPROVEMENT OF EXPERIMENTAL FACILITY

An experimental facility was developed to reproduce the inter-link wear that is induced by the motion of the mooring chain [4]. The specifications of this facility are as follows.

- 1) Two connected studless link chain were adopted as the test objects.
- 2) Constant inter-link force and sliding was applied.
- 3) Experiments were performed in dry air conditions.
- 4) The experiments in this study were performed in dry air condition for the following reason.
  - a) More severe experimental conditions can be achieved in dry air because of abrasion pieces between the links contact surfaces. In seawater, such pieces may be washed away.
  - b) At present, the abrasive wear caused by the sand or gravel embroiled between the link contact surfaces is ignored. The mooring system [5] which we developed for the floating wind turbine behaves similarly to the tensile mooring state. However, the wearing caused by embroiled sand or gravel was observed at the seabed touchdown region in the standard relaxed mooring system [1].

An overview of our experimental facility is shown in Fig. 1. The test links were connected at location [1]. The left link was mounted horizontally and was pulled by the hydraulic equipment, at location [2]. The structure around location [2] is improved to enable applying the initial tensile force even though

the displacement between links increases because of inter-link wear. This overcomes the limitation of our previous experimental facility that had insufficient pulling allowance and the allowance was reduced as the experiment progressed. As a result, the tensile force between links reduced as the progress of inter-link wear. Sliding movement between the links can be achieved by the attached arc-shaped rack and pinion motor, shown at location [3]. The radius of the arc-shaped rack was 588 mm, and the moving arc angle was 90 degrees. One round trip period of the pinion was 243 s. In this improved experimental facility, experimental conditions concerning the inter-link tensile force and the sliding angle can be set for a wide range of values. Only one condition of the inter-link tensile force and the sliding angle could be set in our previous experimental facility.

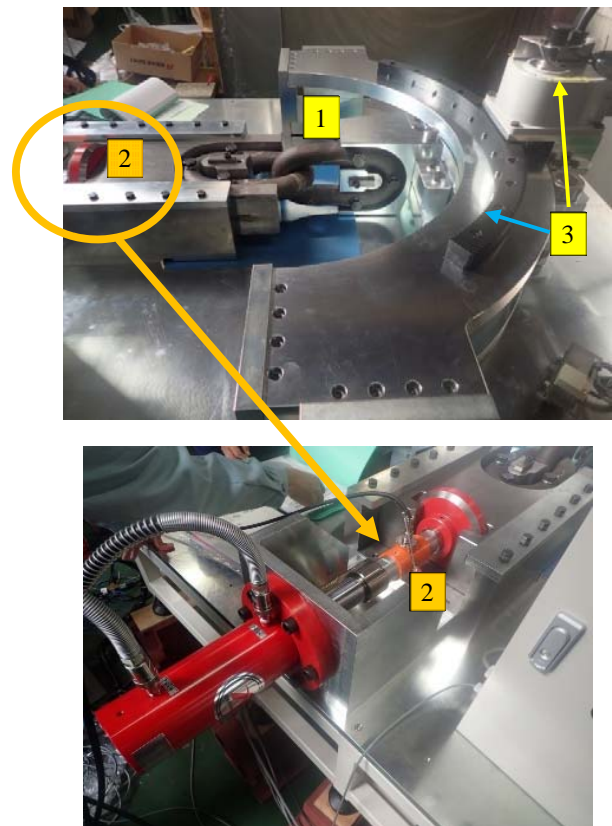


FIGURE 1 OVERVIEW OF MOORING CHAIN WEAR TEST FACILITY.

## WEAR TEST

Wear tests were performed by utilizing the experimental facility described in the previous section. The studless links were made of Grade R3 and R3S classified by ABS [6]. Minimum breaking strength (MBS) of the link was 3,514 kN. The shape of the unit link is shown in Fig. 2.

Test conditions were shown in Table 1. Inter-link tensile force during the first test on Grade R3S link was set as under 40kN, which corresponds to 1.1% of MBS of Grade R3S Studless link. This setting force was decided by referring the

experimental results of our previous research [4]. Applied inter-link tensile force in our previous research was set at 60 kN, which corresponds to 1.7% of the MBS of the link. In our previous experiment, large abraded debris shown in Fig.3 had generated. This debris was still larger than the abrasion powder generated in severe wear and abrasive wear. It is considered that such large abraded debris was generated by the delamination fracture on contact surface because of the large tensile force. In addition, the inter-link contact surfaces had been spreading because the cross section shape of bent section of link is not perfect circle. By considering, mentioned above, applied inter-link tensile forces were set as 40kN or less in this study.

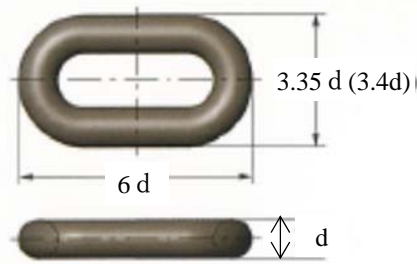


FIGURE 2 SHAPE OF THE STUDLESS LINK ( $d=60\text{mm}$ ).

TABLE 1 TEST CONDITIONS.

Tensile force [kN]:	Grade R3	Grade R3S
	20, 40	20, 30
Sliding angle (deg.):	30 ( $\pm 15$ )	
One round trip period of the pinion (s):	82	
Number of slides performed:	10,000	

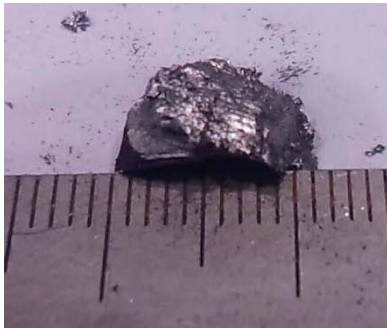
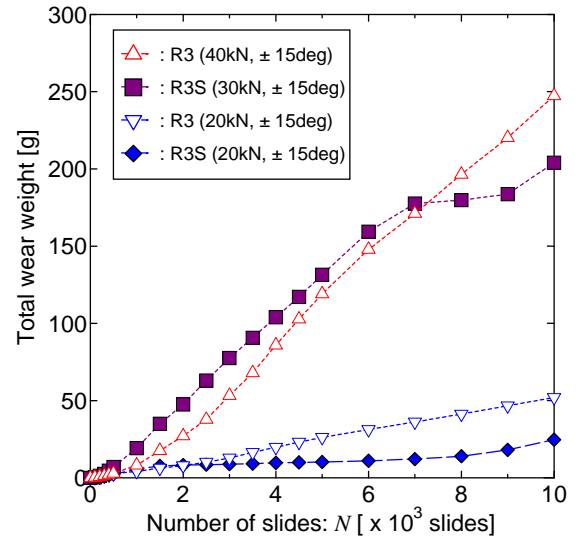


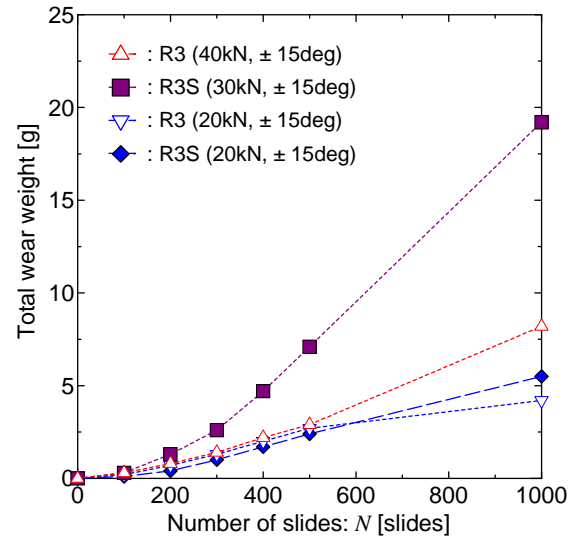
FIGURE 3 LARGE ABRADED PIECE GENERATED AT THE EARLY STAGE OF THE EXPERIMENT.

## WEAR TEST RESULTS

The relationships between the measured total wear weight and number of slides under various inter-link tensile forces are shown in Fig. 4. Examples of observed wear particles generated during the tests are shown in Fig. 5, which includes tensile force of 60kN observed in the previous study [4] for the comparison.



(a) ALL STAGES OF THE EXPERIMENT



(b) ENLARGED VIEW OF THE INITIAL STAGE.

FIGURE 4 COMPARISON OF MEASURED TOTAL WEAR WEIGHT UNDER VARIOUS INTER-LINK TENSILE FORCES.

The appearance of wear particle obtained for inter-link tensile force 60kN, which corresponds to (e) in Fig.5, was different from others. It was silver bright colour and the wear particle size obtained was on the order of millimetre. On the other hand, dark colour and oxidized particles and the size is about 0.1mm were obtained in the other test results. It is confirmed by these appearances of the wear particle that (e) in Fig.5 corresponded to the severe wear and (a) to (d) in Fig.5 were the mild wear. Therefore, the mild wear phenomenon occurred and the severe wear phenomenon did not occur under four inter-link loading conditions shown in Table 1. Then, the weight of

wear particles depended on the tensile force and the material grade, not affected by the type of wear.

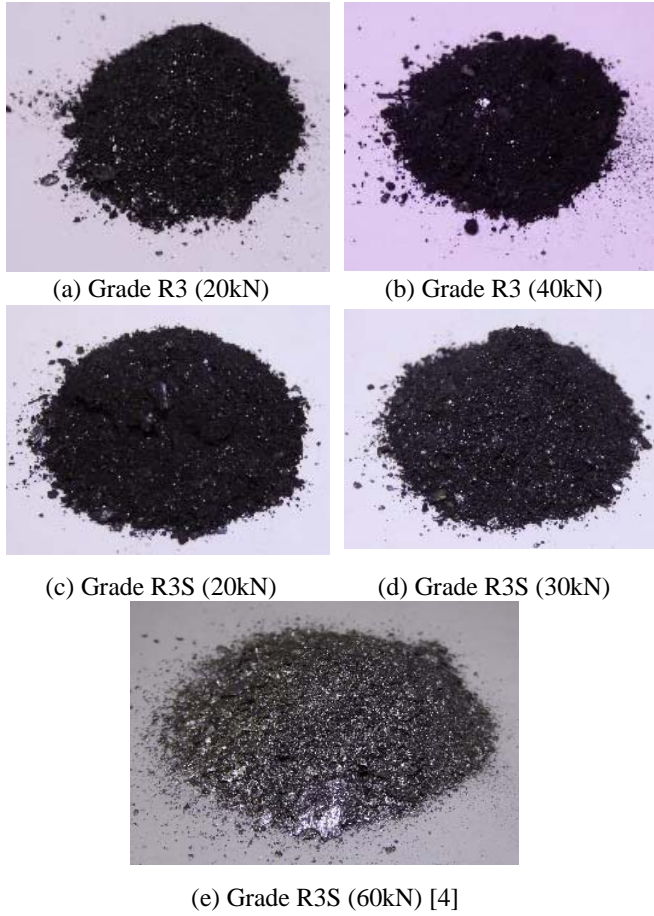


FIGURE 5 COMPARISON OF THE WEAR PARTICLES UNDER VARIOUS INTER-LINK TENSILE FORCES.

Because Grade R3S has higher strength than Grade R3, it is expected that the total wear weight of Grade R3S is less than that of Grade R3. This tendency was observed under inter-link tensile force of 20kN. However, the total wear weight of link made of Grade R3S under inter-link tensile force 30kN was larger than one made of Grade R3 under inter-link tensile force 40kN until about 6,000 slides. This would be the reason why the shape of link bent section is dominant over the material grade and inter-link tensile force. The cross section shape of the link bend is an ellipse rather than a perfect circle. In addition, the degree of flatness of each link varies. Then the contact situation of each applied links were different and affected the degree of wear.

To establish quantitative evaluation of the effect of inter-link tensile force, material grade and shape of link bent section, it is essential to perform quantitative analysis under various experimental conditions.

## REPRODUCTION OF THE EXPERIMENT BY FINITE ELEMENT ANALYSIS

When designing floating wind turbines, the inter-link tensile force and sliding range during the operation can be estimated by a wave response analysis for the floating body. Then the wearing behaviour between links can be estimated from the tensile force and sliding range histories derived from the response analysis.

In previous paper [4] the authors showed that the inter-link wear behaviour could be reproduced numerically by using nonlinear finite element analysis (FEA), including element contact effects and the function of wear phenomenon. To perform an FEA including the wear performance of the materials, the wear coefficient of the material must be identified. The pin-on-disk wearing test, which is a common wear performance test, was performed to obtain the wear coefficient of the material. Uniform rotary motion or rotary reciprocating motion can be used in the pin-on-disk wearing test. In this study, the rotary reciprocating motion was selected to measure the inter-link behaviour. The angle of the rotary reciprocating motion was set to 90 degrees. Values of the wear coefficient in each experiment were identified by the following equations [7]

$$K = HW_s \quad (1)$$

$$W_s = \Delta W / PL\rho \quad (2)$$

where,

- $K$ : Wear coefficient [ $\text{mm}^2/\text{N}$ ],
- $H$ : Vickers hardness,
- $W_s$ : Specific wear rate [ $\text{mm}^2/\text{N}$ ],
- $\Delta W$ : Amount of mass decrease by the wear [g],
- $P$ : Applied load [N],
- $L$ : Sliding distance [mm], and
- $\rho$ : Material density [ $\text{g}/\text{mm}^3$ ].

TABLE 2 WEAR COEFFICIENT OF MATERIALS USED.

Grade	R3	R3S
Maximum value:	$9.12 \times 10^{-4}$	$7.93 \times 10^{-4}$
Minimum value:	$1.48 \times 10^{-5}$	$6.30 \times 10^{-6}$
Average:	$3.66 \times 10^{-4}$	$8.36 \times 10^{-5}$

(Note) unit in  $\text{mm}^2/\text{N}$

Table 2 shows the measured wear coefficient of the link materials. In general, the wear coefficient and the specific wear rate show large scatter. The values shown in Table 3 were derived from 14 times of the pin-on-disk test by using Grade R3 material and 20 times of the test by using Grade R3S material. The amount of scatter in the measured wear coefficient was similar to the results of round robin tests of steels performed by the Japan Society of Mechanical Engineering [8].

The commercial finite element software package MSC Marc 2016 [9] was used in this study. The wear equation



proposed by Archard [10] was implemented in MSC Marc as the governing equation of the wear.

$$W = (K/H) \sigma V_{rel} \quad (3)$$

where,

- $W$ : Wear rate on each finite element node [9] [mm/s],
- $K$ : Wear coefficient [mm<sup>2</sup>/N],
- $H$ : Vickers hardness,
- $\sigma$ : Contact stress on wear surfaces [N/mm<sup>2</sup>] and
- $V_{rel}$ : Relative sliding speed on contact surfaces [mm/s].

Mesh subdivision and model information are shown in Fig. 6. Material constants used in the FEA are shown in Table 3. The contact and shape deformation of bend link section that results from the application of a proof load [12] was not considered in the establishment of FE mesh. Application of an initial proof load could potentially increase the contact area and cause both contact stresses and wear area, which affects the wear computations. This will be considered in future studies.

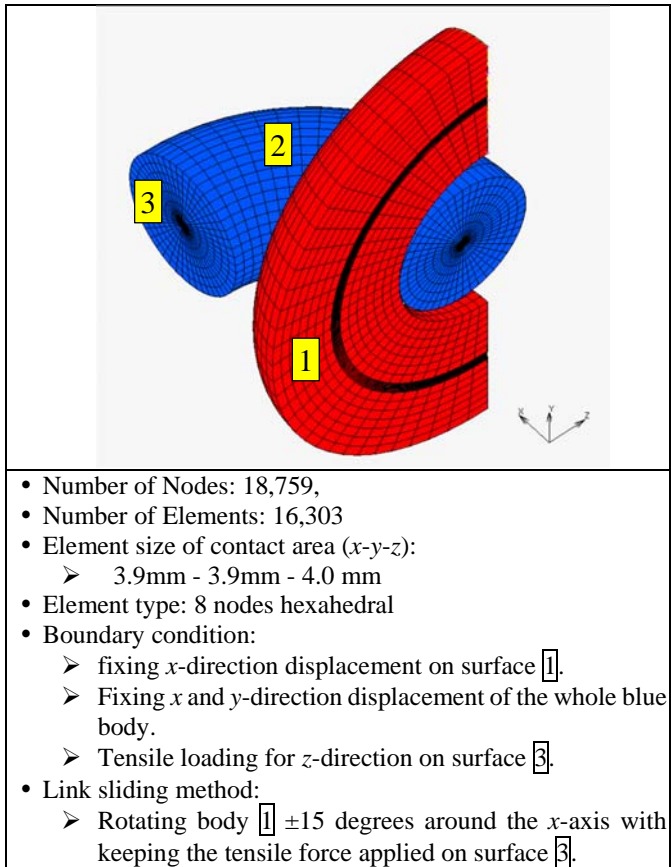
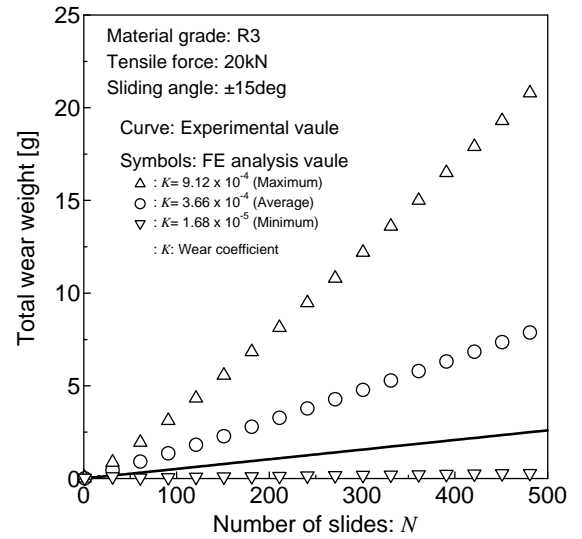


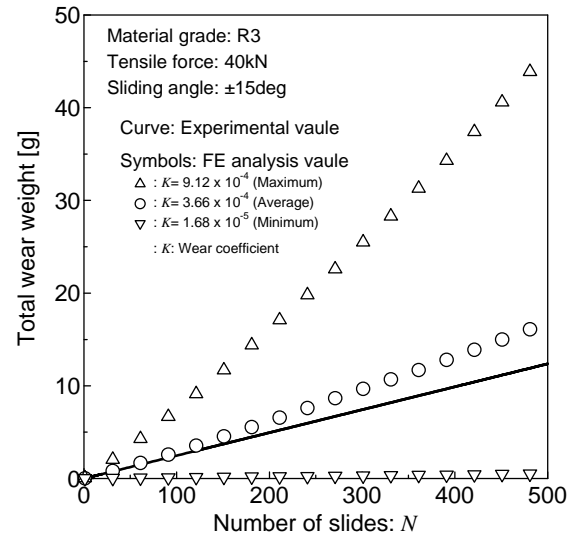
FIGURE 6 FINITE ELEMENT SUBDIVISION AND BOUNDARY CONDCTIONS USED.

TABLE 3 MATERIAL PROPERTIES OF APPLIED LINK.

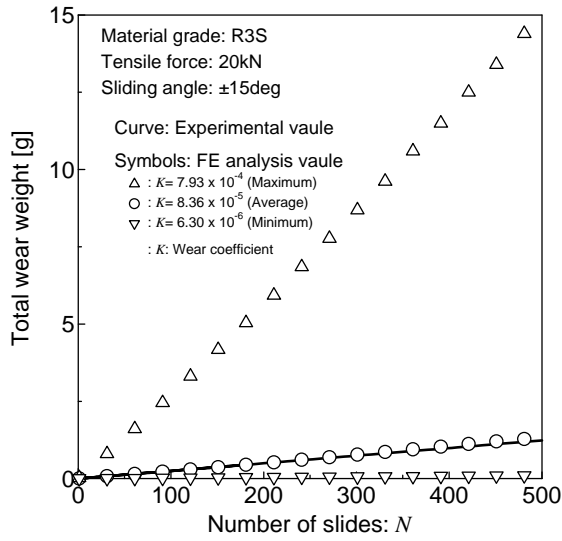
Material grade	R3	R3S
Young's modulus [MPa]:	206,000	
Poisson's ratio:	0.3	
Tensile strength [MPa]:	690	770
Yield strength [MPa]:	410	490
Elongation [%]:	17	15
Density [g/mm <sup>3</sup> ]	7.85 x 10 <sup>-3</sup>	
Vickers hardness [Hv]	275	308



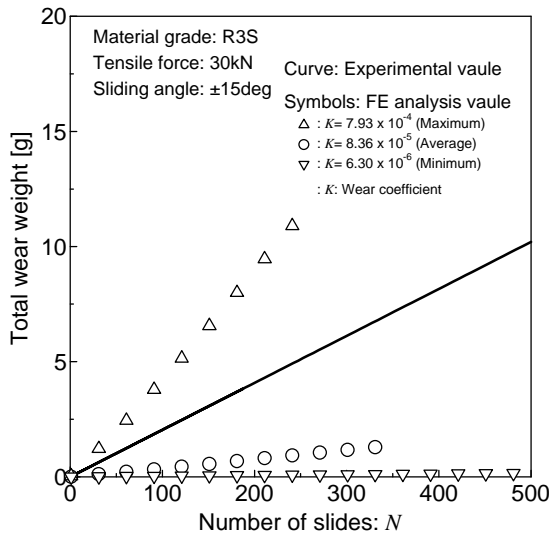
(a) Material Grade: R3, Inter-link tensile force: 20kN.



(b) Material Grade: R3, Inter-link tensile force: 40kN



(c) Material Grade: R3S, Inter-link tensile force: 20kN



(d) Material Grade: R3S, Inter-link tensile force: 30kN

FIGURE 7 WEAR WEIGHT ESTIMATION BY THE FINITE ELEMENT ANALYSIS.

Numerical simulation results were shown in Fig.7. These are the elastic-plastic analysis and the effect of deformation caused by initial tension were considered, i.e. monotonic tensile loading was applied before starting the sliding between links. Three values of the wear coefficient shown in Table 2 were applied in these analyses. Solid curve in each figure corresponds to the average wear weight per one slide during 10,000 slides obtained by the wear tests mentioned in previous section. FE analysis results show values up to 500 slides in Fig.7, because it takes a very long CPU time to perform these FE analysis due to nonlinear analysis and iterative calculation for the convergence are required.

It is concluded from Fig.7 that acceptable FE analysis results were obtained by considering large scattering of measured wear coefficient and that it is recommended to perform FE analysis for estimating the amount of wear weight by using the average value of wear coefficient.

## NUMERICAL STUDY FOR INVESTIGATING INTER-LINK FORCE EFFECT ON WEAR

The validity of nonlinear FE analysis to estimate the wear weight between links was confirmed from the comparison of FE analysis and experimental value shown in Fig.7. In this section, FE analyses with various tensile forces, sliding angles and Vickers hardness value were performed in order to investigate the effect of these variables. In these numerical analysis, material grade was set to R3S and average value of the wear coefficient was applied. FE analysis results were performed up to 500 slides.

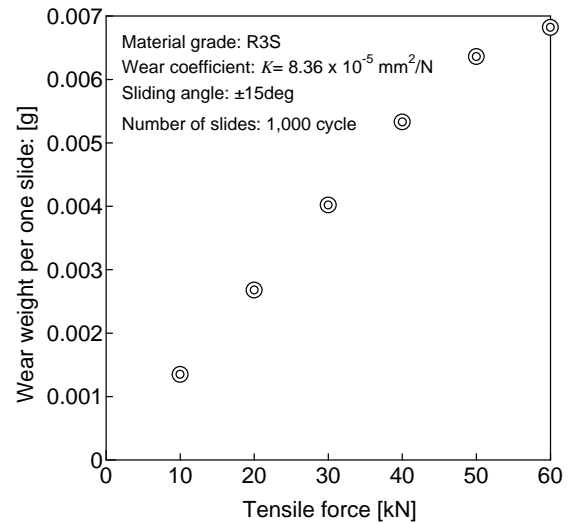


FIGURE 8 RELATIONSHIP BETWEEN THE WEAR WEIGHT PER ONE SLIDE AND THE TENSILE FORCE BY FINITE ELEMENT ANALYSIS.

Figure 8 shows the relationship between inter-link tensile force and wear weight per one slides. Sliding angle was set to  $\pm 15$  degree for all FE analysis. It is confirmed from Fig. 8 that the amount of wear weight is proportional to the inter-link forces. However, such linear relation has begun to disappear near the tensile force of 60kN. One of the reasons might be insufficient FE simulation. By referring Fig.5, it is confirmed that the wear phenomenon changes from the mild wear to the severe wear when the inter-link tensile force reaches near 60 kN. However, the wear coefficient applied in the FE analysis was obtained under the mild wear condition and the severe wear phenomenon cannot reproduced by FE analysis until now. Then, numerical results for inter-link tensile force of 60kN seems to be inferior in reliability compared with other results.

Figure 9 shows the relationship between inter-link sliding angle and wear weight per one slides. Inter-link tensile force was

set to 20kN for all FE analysis. It is confirmed from Fig. 9 that the amount of wear weight is proportional to the inter-link sliding angle. Since the actual behaviour of inter-link sliding does not exceed  $\pm 45$  degrees, it can be considered that the wear amount is proportional to the inter-link sliding angle.

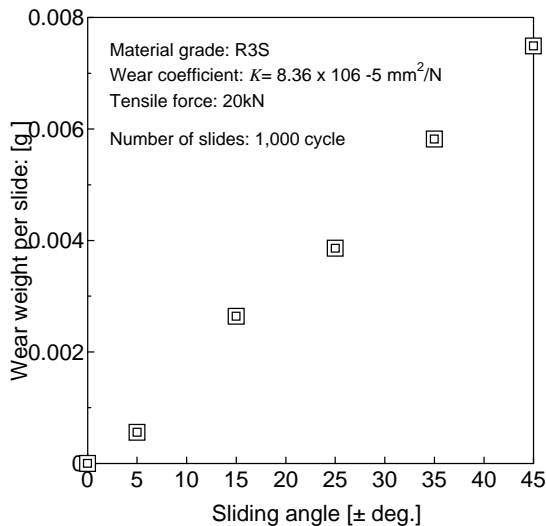


FIGURE 9 RELATIONSHIP BETWEEN THE WEAR WEIGHT PER ONE SLIDE AND THE SLIDING ANGLE BY FINITE ELEMENT ANALYSIS.

## CONCLUSIONS

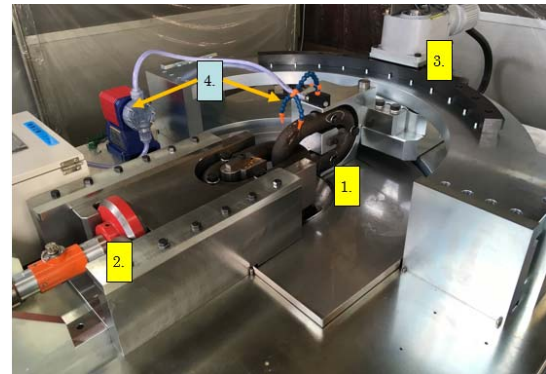
The experimental facility proposed by authors in the previous research was improved to reproduce inter-link wear in actual scale. FEA was used to reproduce the phenomenon of inter-link wear and the early stage of the experiment was successfully reproduced. In addition, numerical simulations of the inter-link wear were performed to investigate the effect of inter-link tensile force and sliding angle on the amount of wear. It is confirmed that the amount of wear is proportional to the inter-link sliding angle under actual range of inter-link sliding and that the amount of wear is proportional to the inter-link tensile force when the wear phenomenon satisfy the mild wear.

Future challenges are as follows.

- 1) Improvement of the FE analysis procedure to reproduce the inter-link wear under long period and variable tensile force and sliding angle conditions.
- 2) Improvement of our experimental facility so that the wear test in actual scale can be performed under seawater environment. Figure 10 is our new experimental facility, which we are currently developing, the inter-link contact region is exposed to seawater. We will report on the experiments by using this improved experimental facility at next opportunity.

## ACKNOWLEDGMENTS

This research was supported by the Low Carbon Technology Research and Development Program (FY2015-FY2017), Ministry of the Environment, Japan.



- [1]~[3]: The same as shown in Fig.1
- [4] Pumping system to drop seawater on the inter-link contact region.

FIGURE 10 OVERVIEW OF IMPROVED MOORING CHAIN WEAR TEST FACILITY.

## REFERENCES

- [1] Aso, Y. and Hashimoto, S., 2015, Strength and wear characteristics of the buoy mooring chain, Bulletin of JASNAOE, 62, pp.11-14 (in Japanese).
- [2] Yaghim, A.L. and Melchers, R.E., 2015, Long-term inter-link wear of model mooring chains, Marine Structures, 44, pp.61-84.
- [3] Brown, M.G., Comley, A.P., Eriksen, M., Williamns, I., Smedley, P., Bhattacharjee, S., 2010, Phase 2 Mooring Integrity JIP -Summary of Findings, Proceedings of OTC, OTC 20613.
- [4] Gotoh, K., Murakami, K. Nakagawa, M. and Utsunomiya, T., 2017, Experimental Study on the Wear Performance of the Mooring Chain, Proceedings of OMAE 2017, OMAE2017-62195.
- [5] Utsunomiya, T., et al., 2015, Design and Installation of a Hybrid-spar Floating Wind Turbine Platform, Proceedings of OMAE 2015, OMAE2015-41544.
- [6] American Bureau of Shipping, 1999, Guide for Certification of Offshore Mooring Chain.
- [7] For example, Sasada, T., 2008, Wear, Yokendo, ISBN: 978-4-8425-0433-9 (in Japanese).
- [8] Japan Society of Mechanical Engineering, 2010, JSME S013-2010: Standard test procedure of the wear, pp.38-52.
- [9] <http://www.mscsoftware.com/product/marc> (Accessed on January 4, 2018.)
- [10] Archard, J.A., 1956, Contact and Rubbing of Flat Surface, J. of Applied Physics, 24, pp. 981-988.
- [11] MSC Marc 2015 Manual Volume A: Theory and User Information, 2015, pp.210-212.
- [12] Vargas, P.M. and Jean, P., 2005, FEA of Out-of-Plane Fatigue Mechanism of Chain Links, Proceedings of OMAE 2005, OMAE2005-67354.